

Magnetocaloric Effect in Two-Dimensional Diluted Ising Model: Appearance of Frustrations in the Ground State

A.V. Shadrin^{a,*}, V.A. Ulitko^a, Y.D. Panov^a

^aUral Federal University Named after the First President of Russia B.N. Yeltsin,

Yekaterinburg, Russia

* e-mail: shadrin.anton@urfu.ru

Abstract

The magnetocaloric effect in a two-dimensional Ising model is considered for different ratios between parameters of inter-site repulsion of nonmagnetic impurities and exchange coupling. Classical Monte Carlo simulations on a square lattice show that in case of weak coupling and at sufficiently high concentrations of nonmagnetic impurities the long-range ferromagnetic ordering breaks down to give isolated spin clusters in the ground state of the system. This leads to appearance of a paramagnetic response in the system at the zero temperature and nonzero entropy of the ground state. The feasibility to detect frustration of ground state using data on the magnetic entropy variation is discussed.

1 Introduction

The magnetocaloric effect (MCE) consists in release or absorption of heat as a result of variation of an external magnetic field applied to a material. Initially, the effect was used to reach temperatures below 1 K, but, since materials exhibiting MCE at near room temperature have been discovered, magnetic cooling has become an area of very active research. The MCE in frustrated and low-dimensional systems attracts a special interest [1, 2, 3, 4]. In Ising-type two-dimensional systems, the dependence of MCE on the parameter of magnetoelastic interaction for a square lattice was investigated in [5], while the effects of shape and size of geometrically frustrated

Ising spin clusters in a triangular lattice have on the MCE were addressed in [6]. In this work, we consider a two-dimensional Ising system with a fixed concentration of mobile nonmagnetic charged impurities. The dilute Ising model is one key model [7, 8] in the theory of magnetic systems with quenched or annealed disorder as well as in the thermodynamic theory of binary alloys and mixtures of classical and quantum liquids. To describe our system, we use the pseudo-spin formalism ($S = 1$) in which for a given lattice site the states with pseudo-spin projections $S_z = \pm 1$ correspond to two magnetic states with spin projections $s_z = \pm 1/2$, while the state with $S_z = 0$ corresponds to a charged nonmagnetic impurity. Write the Hamiltonian as follows:

$$H = -\tilde{J} \sum_{\langle ij \rangle} S_{zi} S_{zj} + V \sum_{\langle ij \rangle} P_{0i} P_{0j} - h \sum_i S_{zi}, \quad (1)$$

where S_{zi} is the z -projection of pseudo-spin operator on a site, $P_{0i} = 1 - S_{zi}^2$ is the projection operator on state $S_{zi} = 0$, $\tilde{J} = Js^2$, J is an exchange integral, $s = 1/2$, V is the inter-site interaction between impurities, h is an external magnetic field, $\langle ij \rangle$ – are the nearest neighbors, and the sum is taken over all sites of the twodimensional square lattice. The concentration n of charged nonmagnetic impurities is fixed so that $nN = \sum_i P_{0i} = const$, where N is the number of lattice sites.

The system described by Hamiltonian (1) exhibits two types of phase diagrams that are exemplified in Fig. 1. An example with a strong coupling ($\tilde{J} > V$) is shown in the left panel (Fig. 1a). As the temperature is lowered, two consecutive phase transitions occur in the system in the range of $0 < n < 0.6$. The first one is a transition from a high-temperature disordered state into ordered ferromagnetic (FM) one diluted with randomly distributed charged impurities. At low temperatures, mobile charged impurities condense into "drops". This means that in case of strong coupling the dilute FM phase is unstable with respect to phase separation (PS) when the FM matrix expels impurities in order to minimize surface free energy associated with them. Weak coupling, i.e., when $\tilde{J} < V$, is exemplified in the right panel (Fig. 1b). With the impurity concentration increasing, the FM spin ordering

transforms into charge ordering (CO) of nonmagnetic impurities. Further, we limit our discussion to the range of $0 < n < 0.5$, because for $n > 0.5$ there is no long-range order in a spin system with a fairly high critical temperature.

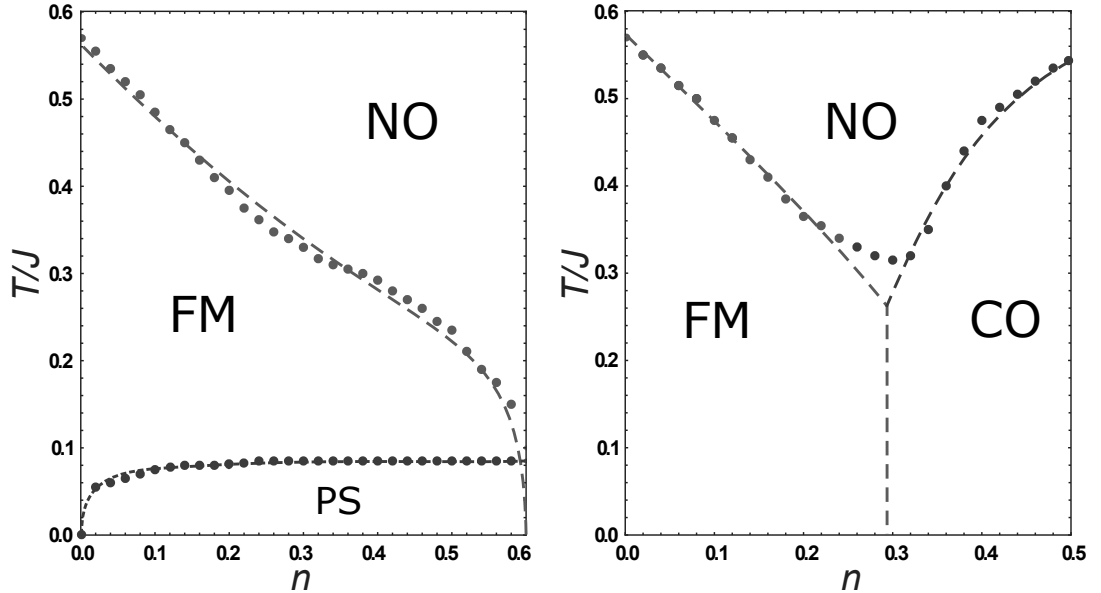


Fig. 1: Phase diagrams for the system with Hamiltonian (1): (a) $V/\tilde{J} = 0.4$ (strong coupling) and (b) $V/\tilde{J} = 4$ (weak coupling). The temperatures corresponding to maximum heat capacity values, as calculated by a Monte Carlo method, are shown with filled circles. Dotted lines schematically indicate boundaries of disordered (NO), ferromagnetic (FM), and charge-ordered (CO) phases, as well as a phase separation region (PS).

The competition between magnetic and charge orders can be implemented in systems subject to disproportionation or instability with respect to charge transfer fluctuations [9], e.g., as in cuprates. Typically, with concentration n of impurities increasing, the magnetic ordering is broken, the critical temperature is lowered, and the temperature corresponding to maximum values for MCE parameters, such as isothermal variation of magnetic entropy and adiabatic temperature variation, is lower as well. Changes in the maximum MCE temperature related to changes in the chemical composition have been well demonstrated in [10, 11, 12]. However, the phase state of the system described by Hamiltonian (1) also depends on the ratio between the constants of exchange and density–density interactions, as was shown for a similar spin–pseudo-spin model [13, 14, 15, 16]. In this work, we compare the MCE parameters in cases of strong and weak coupling; we also explore the

possibility of detecting frustration in ground state of the system with weak coupling using magnetic entropy data.

2 Calculation procedure for the MCE parameters using Monte Carlo data

The adiabatic temperature change ΔT_{ad} and isothermal magnetic entropy change ΔS_M are the key parameters characterizing MCE. ΔS_M is calculated by the equation:

$$\Delta S_M(T, h) = \int_0^T \frac{C(T', h_m) - C(T', 0)}{T'} dT', \quad (2)$$

where C is a heat capacity. Maxwell relationship $(\partial S/\partial h)_T = (\partial M/\partial T)_h$ gives us another expression for ΔS_M and an equation for ΔT_{ad} :

$$\Delta S_M(T, h_m) = \int_0^{h_m} \left(\frac{\partial M(T, h)}{\partial T} \right)_h dh \quad (3)$$

$$\Delta T_{ad}(T, h_m) = \int_0^{h_m} \frac{T}{C(T, h)} \left(\frac{\partial M(T, h)}{\partial T} \right)_h dh, \quad (4)$$

where M is a magnetization and h is an external magnetic field. In case of second-order phase transitions, expressions (2) and (3) must lead to identical results. Further, magnetic field and temperature are expressed in energy units, and entropy is expressed in k_B units.

To obtain temperature dependences of MCE parameters for the system with Hamiltonian (1), we used the Metropolis algorithm within the classical Monte Carlo method. Calculations were carried out for a 64×64 square lattice with periodic boundary conditions. In our program, we ensured that the condition for a constant concentration of impurities, i.e., $nN = \sum_i P_{0i} = \text{const}$, is held, since the variation in the state of an arbitrarily chosen pair of lattice sites a and b was performed while

sum $P_{0a} + P_{0b}$ was held constant.

We implemented a variant of this algorithm for parallel computations using NVIDIA graphic accelerators, which enabled us to perform calculations for 64 copies of the system simultaneously. For each system copy, we lowered the temperature, while keeping the external magnetic field constant, from value $T_1/J = 1.0$, which is around twice the magnetic ordering temperature, to $T_0/J = 0.01$ at a step of $T/J = 0.01$. We then varied the external magnetic field from $h/J = 0$ to $h_m/J = 0.04$ at a step of $h/J = 0.001$. Modeling was performed for impurity concentration $0 < n < 0.5$ at a step $n = 0.1$. For each value for n , T and h we obtained average values for energy, specific heat C and magnetization M . This allowed us to use the trapezium rule for discretization of integrals and a threepoint method for derivative $(\partial M/\partial T)_h$ in Eqs.(2)–(4).

With Eqs. (2) and (3), we can calculate the variation of magnetic entropy using different Monte Carlo data, i.e., the specific heat and magnetization. The results of these calculations are in fairly good agreement in case of strong coupling ($\tilde{J} > V$) but at variance in case of weak coupling ($\tilde{J} < V$). This is shown in Fig. 2 for impurity concentration $n = 0.3$.

In contrast to the case of strong coupling, with a strong density–density interaction between impurities ($V > \tilde{J}$), the value of paired distribution function for the nearest neighbors turns 0 at a sufficiently low temperature and leads to charge ordering for $n \geq 0.3$. A picture characteristic of such charge ordering is shown in Fig.3. As a result, isolated spin clusters surrounded by nonmagnetic impurities are formed. These clusters behave like paramagnetic centers and furnish additional contribution S_0 to the system entropy at the zero temperature. The simplest estimation of this contribution can be based on the equation

$$S_0 = N_{cl} \ln 2, \tag{5}$$

where N_{cl} is the number of isolated spin clusters. To determine average number of

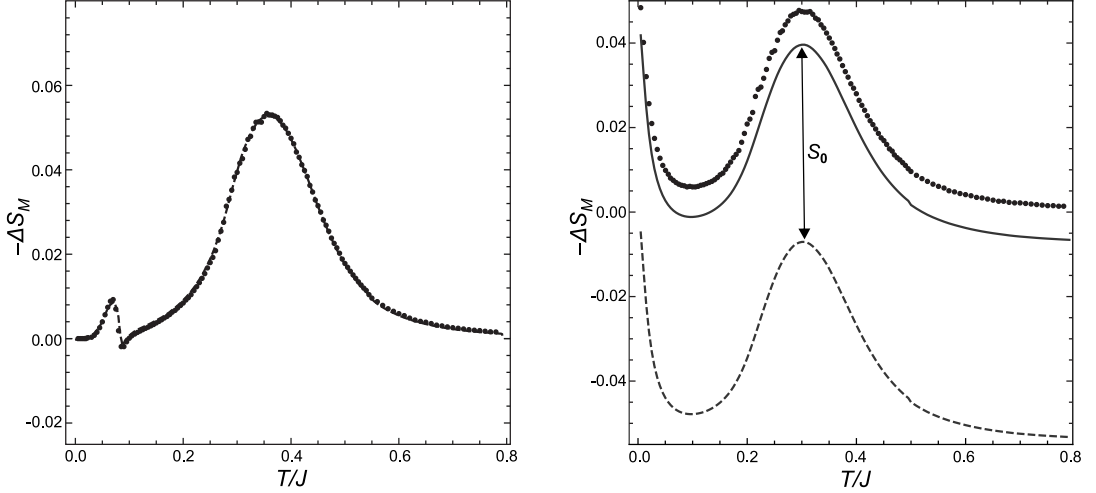


Fig. 2: Magnetic entropy change for $n = 0.3$ in the case of (a) strong coupling ($V/\tilde{J} = 0.4$) and (b) weak coupling ($V/\tilde{J} = 4$). Results of calculations carried out using Eqs.(2) and (3) are shown with dotted lines and filled circles, respectively. A continuous line pertaining to the case of weak coupling takes into account a contribution calculated by Eq.(6). The value corresponds to the average concentration of paramagnetic clusters for $n = 0.3$ shown in Fig. 3.

clusters on a 64×64 , lattice, we used a separate program that generated random distributions of charged impurities having a minimal energy. The results of calculations are presented in Fig.3. Considering the contribution given by Eq.(5), formula (2) reads

$$\Delta S_M(T, h) = S_0 + \int_{T_{min}}^T \frac{C(T', h_m) - C(T', 0)}{T'} dT', \quad (6)$$

where T_{min} is the minimum temperature used in Monte Carlo simulations. As is shown in Fig.2, this improved consistency with ΔS_M , M dependence that was calculated using Eq.(3). Thus, differences in results of magnetic entropy ΔS_M measurements that were obtained through Eqs.(2) and (3) may point to some hidden frustrations in the system.

3 Results

The dependence of isolated cluster concentration and the difference between maximum values for magnetic entropy change ΔS_M as calculated by Eqs. (2) and (3) and

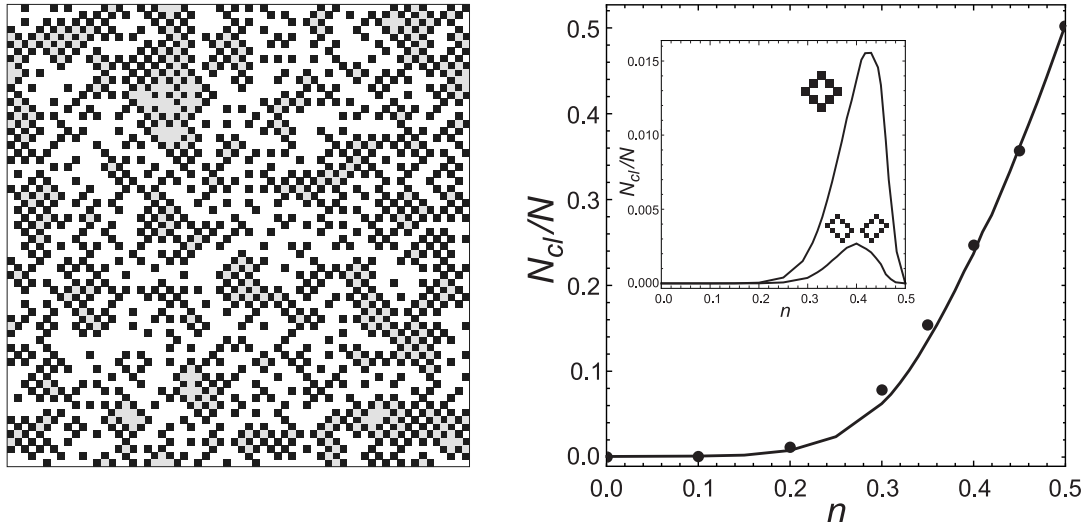


Fig. 3: (a) Snapshot showing a configuration of the ground state for $n = 0.3$ and $V/\tilde{J} = 4$ (weak coupling). Lattice sites with $S_z = 1$ and $S_z = -1$ are represented by white and light-grey squares, respectively. Positions of nonmagnetic impurities ($S_z = 0$) are designated with black squares. (b) Average concentration of isolated paramagnetic clusters on a 64×64 lattice. Inset: the results for clusters comprised of 5 and 8 spins. The difference between maximum values for magnetic entropy variation ΔS_M , as calculated using Eqs.(2) and (3) and expressed in the units of average concentration of clusters (Eq.(5)), is shown with filled circles.

expressed in the units of average concentration, are presented in Fig.3. We highlight a good agreement between the cluster concentration and the frustration data for the ground state of the system obtained from MCE. Partial contribution of clusters consisting of 5 and 8 spins are shown in the inset to this figure. The maximum values for these contributions are an order of magnitude lower than the total concentration of isolated paramagnetic clusters for a given n , which draws us to a conclusion that smallest clusters, including 1 spin, make a decisive contribution to the ground state entropy. In this case, the concentration of smallest paramagnetic clusters increases monotonically with increasing n reaching maximum $N_{cl}/N = 0.5$ at $n = 0.5$.

Using a discrete approximation for Eqs. (3) and (4) we calculated isothermal magnetic entropy change ΔS_M and adiabatic temperature change ΔT_{ad} on the basis of Monte Carlo data. The results for ΔS_M and ΔT_{ad} in the case of strong coupling, i.e., $V/\tilde{J} = 0.4$, for $n = 0.0, 0.1, 0.2, 0.3, 0.4$ are shown in Fig.4. The temperatures corresponding to maximum values for the two parameters follow approximately the

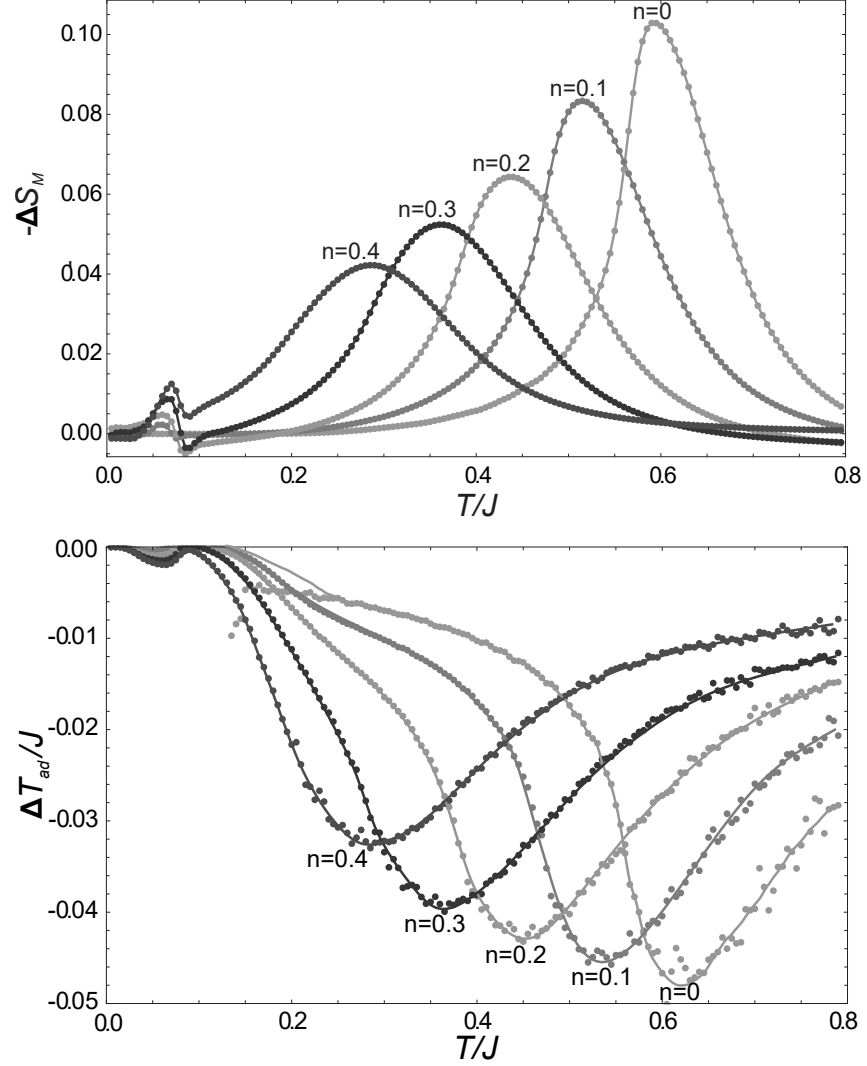


Fig. 4: Magnetic entropy change ΔS_M and adiabatic temperature change ΔT_{ad} for concentrations n of nonmagnetic impurities in the range of $0 \sim 0.4$ in case of strong coupling ($V/\tilde{J} = 0.4$).

variation of magnetic ordering temperature with n . The peak width grows, while their height diminishes as n increases, because of impurity-induced smearing of the phase FM transition. At low temperatures, dependences ΔS_M and ΔT_{ad} feature an additional peak caused by phase separation. ΔS_M and ΔT_{ad} in the case of weak coupling, i.e., $V/\tilde{J} = 4$, for $n = 0.0, 0.1, 0.2, 0.3, 0.4, 0.5$ are shown in Fig.5. For $n = 0.0$ and $n = 0.1$, these results are nearly identical to those for strong coupling. However, qualitative differences are seen at $n > 0.1$, especially at low temperatures. As was discussed above, charge ordering in the impurity subsystem leads to the formation of isolated spin clusters. This causes a paramagnetic response

of the MCE parameters that gives maximum value $\Delta T_{ad}/J \approx 0.55$ for $n = 0.5$ and $T/J = 0.14$.

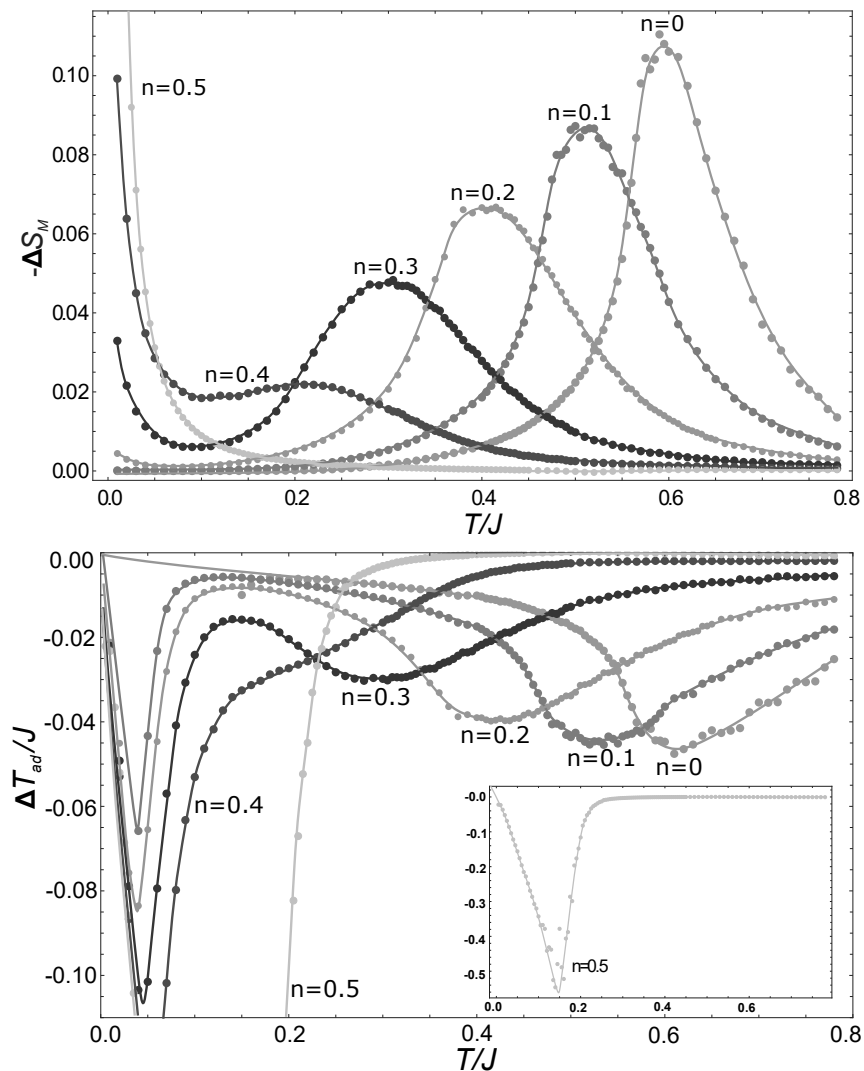


Fig. 5: Magnetic entropy change ΔS_M and adiabatic entropy change ΔT_{ad} for concentrations n of nonmagnetic impurities in the range of $0 \sim 0.5$ in case of weak coupling ($V/\tilde{J} = 4$). Inset: results for $n = 0.5$.

4 Conclusions

We performed Monte Carlo simulations of a twodimensional Ising system containing a fixed concentration of mobile nonmagnetic charged impurities, which enabled us to construct temperature dependences of the MCE parameters. It was shown that in case of weak coupling, for nonmagnetic impurity concentration $n > 0.1$, isolated

spin clusters are formed in the ground state of the system. This leads to nonzero entropy of the system's ground state. The feasibility to detect a frustration in the ground state is demonstrated using the magnetic entropy variation data. The MCE parameters were calculated for the cases of strong and weak coupling.

Funding

The work was supported within the Competitiveness Enhancement Program of the Ural Federal University (Russian Federation Government Act 211, agreement no. 02.A03.21.0006), by the Ministry of Education and Science, Russian Federation (project FEUZ–2020 – 0054), and by the Russian Foundation for Basic Research (research project no. 18 – 32 – 00837\18).

Conflict of interest

The authors declare that they have no conflicts of interest.

References

- [1] M. E. Zhitomirsky. Phys. Rev. B **67**, 104421 (2003).
- [2] M. E. Zhitomirsky, A. Honecker. J. Stat. Mech.: Theory Exp. **2004**, P07012 (2004).
- [3] A. Honecker, S. Wessel. Physica B **378-380**, 1098 (2006).
- [4] B. Schmidt, P. Thalmeier, N. Shannon. Phys. Rev. B **76**, 125113 (2007).
- [5] J. S. Amaral, J. N. Goncalves, V. S. Amaral. IEEE Trans. Magn. **50**, 1 (2014).
- [6] M. Žukovič. J. Magn. Magn. Mat. **374**, 22 (2015).
- [7] S. Katsura, B. Tsujiyama. Ferro- and Antiferromagnetism of Dilute Ising Model, in: C. Domb (Ed.), Proceedings of the Conference on Phenomena in the Neighborhood of Critical Points, National Bureau of Standards, Washington, D.C., 1965, pp. 219–224.
- [8] M. Blume, V. J. Emery, R. B. Griffiths. Phys. Rev. A **4**, 1071 (1971).
- [9] A. S. Moskvina. J. Phys.: Condens. Matter **25**, 085601 (2013).
- [10] B. G. Shen, J. R. Sun, F. X. Hu, H. W. Zhang, Z. H. Cheng. Adv. Mater. **21**, 4545 (2009).
- [11] A. A. Inishev, E. G. Gerasimov, N. V. Mushnikov, P. B. Terent'ev, V. S. Gaviko. Physics of Metals and Metallography **119**, 1036 (2018).
- [12] H. Zhang, R. Gimaev, B. Kovalev, K. Kamilov, V. Zverev, A. Tishin. Physica B **558**, 65 (2019).
- [13] Y. D. Panov, A. S. Moskvina, A. A. Chikov, I. L. Avvakumov. J. Low Temp. Phys. **185**, 409 (2016).

- [14] Y. D. Panov, A. S. Moskvina, A. A. Chikov, I. L. Avvakumov. Journal of Superconductivity and Novel Magnetism **29**, 1077 (2016).
- [15] Y. D. Panov, K. S. Budrin, A. A. Chikov, A. S. Moskvina. JETP Letters **106**, 440 (2017).
- [16] Y. Panov, V. Ulitko, K. Budrin, A. Chikov, A. Moskvina. J. Magn. Magn. Mat. **477**, 162 (2019).